

## Condensation of vapours of immiscible liquids in the presence of a non-condensable gas

Christian Mönning<sup>a\*</sup>, Rainer Numrich<sup>b</sup>

<sup>a</sup> University of Paderborn, FB 10, Process Engineering, Warburger Straße. 100, 33098 Paderborn, Germany

<sup>b</sup> Gebr. Lödige Maschinenbau GmbH, Geschäftsbereich Umwelttechnik, Elsener Straße. 7–9, 33102 Paderborn, Germany

(Received 29 June 1998, accepted 26 January 1999)

**Abstract** — During partial condensation of vapours from a mixture with non-condensing gas, the gas content causes a resistance to heat and mass transfer. If the two vapour components are immiscible in the liquid state, at each composition except from the heteroazeotrope, usually called eutectic composition in analogy with solid/liquid systems, one vapour component will additionally behave as a non-condensing gas. Only when this azeotropic composition is obtained at the gas/liquid interface, will the two vapour components condense simultaneously. Whereas conventional methods can be used to calculate the heat and mass transfer coefficients in the gas phase, transport mechanisms are insufficiently described due to the inhomogeneity of the two-phase condensate. For this reason, in the past, only simplified calculations, based on idealised model forms of condensation, were generally used. Following our own visual examination, calculation using the model of a homogeneously mixed condensate was favoured. For the first time tests were performed using this type of condensation at pressures above atmospheric and at gas-Reynolds numbers above 25 000, and up to 240 000. It was discovered that the turbulent hydrodynamic conditions of the tests allow the calculation with the simple calculation methods mentioned above. Good results were produced with an accuracy of  $\pm 20\%$  in nearly all experiments. Where there is a water surplus in the condensate, excessively high water condensate massflow rates were systematically predicted. If there was a heptane surplus, the heptane flow rate was underpredicted. © Elsevier, Paris.

condensation / immiscible liquids / non-condensing gas / modelling / eutectic / azeotropic / mass and heat transfer

**Résumé** — Condensation de vapeurs provenant de liquides immiscibles en présence d'un gaz inerte. Lors de la condensation partielle d'un mélange de gaz/vapeur, le gaz constitue une résistance pour l'ensemble du transfert de chaleur et de matière. Si le mélange est constitué de vapeurs dont les liquides sont insolubles, chaque vapeur se comporte pour l'autre comme un gaz inerte, sans tenir compte de la composition eutectique. C'est seulement pour cette composition eutectique que les deux vapeurs se condensent en même temps. Alors que pour calculer le transfert de chaleur et de matière dans la phase gazeuse on peut se référer à des mécanismes connus, ceux qui ont lieu dans le cas d'un condensat à deux phases ne peuvent être décrits que de manière insuffisante, en raison du manque d'homogénéité de ce condensat. On a donc été obligé, jusqu'à maintenant, pour faire ce calcul, de se référer à des mécanismes moyens et simplifiés, basés sur une représentation type idéalisée des formes de condensation. À partir d'observations expérimentales, nous proposons un modèle de condensation mélangée homogène. Pour la première fois, des essais ont été réalisés pour ce type de condensation sous pression très élevée et des nombres de Reynolds de gaz de 25 000 à 240 000. Il est apparu que les conditions hydrodynamiques dominantes dans ce cas permettent un calcul avec des méthodes de moyenne déjà citées et donnent de bons résultats, tant que la composition gaz/vapeur reste proche de celle du point eutectique. Pour les compositions non eutectiques, un débit massique trop élevé est systématiquement calculé. © Elsevier, Paris.

condensation / liquides immiscibles / gaz incondensable / modélisation / eutectique / azéotrope / transfert thermique / transfert de masse

### Nomenclature

$\bar{c}_p$  av. specific heat capacity .....  $\text{J}\cdot\text{kg}^{-1}\cdot\text{K}^{-1}$   
 $C_m$  correction factor

$C_q$  correction factor  
 $d$  tube diameter ..... m  
 $D$  diffusion coefficient .....  $\text{m}^2\cdot\text{s}^{-1}$   
 $fr$  degrees of variance  
 $\Delta h_v$  evaporation enthalpy .....  $\text{J}\cdot\text{kg}^{-1}$   
 $L$  length ..... m  
 $l$  number of substances

\* Correspondence and reprints.  
jmoen1@vt.uni-paderborn.de

$\dot{m}$	mass flux .....	$\text{kg}\cdot\text{s}^{-1}\cdot\text{m}^{-2}$
$\dot{M}$	mass flow .....	$\text{kg}\cdot\text{s}^{-1}$
$\bar{M}$	molar mass .....	$\text{kg}\cdot\text{mol}^{-1}$
$Nu$	Nusselt number	
$p$	pressure .....	Pa
$Pr$	Prandtl number	
$\dot{q}$	heat flux .....	$\text{J}\cdot\text{s}^{-1}\cdot\text{m}^{-2}$
$Re$	Reynolds number	
$Sh$	Sherwood number	
$T$	temperature .....	K
$x$	mass fraction in liquid	
$\hat{x}$	volume fraction in liquid	
$\tilde{x}$	mole fraction in liquid	
$\tilde{y}$	mole fraction in gas phase	
$z$	cooling length .....	m
<i>Greek symbols</i>		
$\alpha$	heat transfer coefficient .....	$\text{m}^2$
$\beta$	mass transfer coefficient .....	$\text{m}\cdot\text{s}^{-1}$
$\gamma$	activity coefficient	
$\Delta$	difference	
$\vartheta$	temperature .....	$^{\circ}\text{C}$
$\lambda$	thermal conductivity	
$\pi$	constant	
$\xi$	roughness factor	
$\Phi$	number of phases	
<i>Subscripts</i>		
c	cooling medium	
e	eutectic	
E	entry	
exp	experimentally	
g	smooth	
G	gas phase	
O	phase boundary	
$i$	component number	
I	inert gas	
$j$	component number	
L	liquid phase	
max	maximum	
n	number of all components	
r	rough	
th	theoretically	
0	starting point	
1	component heptane	
2	component water	

## 1. STARTING POSITION AND OBJECTIVE

At the beginning of this research there were no results available from experiments made under relevant practical conditions for the partial condensation of components from a gas/vapour mixture where they are immiscible in the liquid form. Only two studies [1, 2] were found which handled the effect of non-condensing gas during

condensation of this system. The testing equipment previously used by these and other authors made testing at pressures above 1 bar or with highly turbulent condensate flow ( $Re_L > 150$ ) impossible.

The conditions described above are, however, frequently used in processes in the chemical and petrochemical industries. In these cases, the process of condensation is frequently run under high pressure in vertical tube bundles, in which turbulent flow conditions of the gas and liquid phases are the general rule.

When immiscible liquids are present, e.g. as produced in carrier distillation caused by downstream condensation, it is very important to determine the heat transfer in the two-phase condensate. The calculations used for designing such heat exchangers are very unsafe, even under ideal conditions (small apparatus, laminar flow, and no influence of pressure or non-condensing gas). The two calculations most used [3, 4] are based on extremely simple model concepts of the forms of condensate produced. Essentially they represent a combination of drop and film condensation. Sardesai [1, 5] compared in his work the two said models and found systematic variations of 0–50 %.

These two models were initially used as a basis for predicting the conditions aimed at in this study. The literature provides conflicting descriptions of the visual examination under diverse working conditions on small condenser surfaces, leaving us to assume that many forms of condensation occur in parallel or consecutively in an industrial condenser. It therefore appeared sensible to undertake and observe our own experiments over an extended section of a condenser surface.

A proven pilot plant was available for the main condensation tests under high pressure. The plant was modified to include an additional material circulation for the use of immiscible materials. Evaluation of the test results was carried out (under consideration of the local heat and mass transfer coefficients) with the help of a step-by-step computer program. New, validated correlations [6–8] are available for the calculation of the mass and heat transport in the gas phase.

At pressures above atmospheric, it is important to include the shear stress at the phase boundary, which promotes the exchange processes in the gas and liquid phases, and also to model the real behaviour in the gas phase. The mass transfer is determined by a considerably simplified method based on the use of an effective diffusion coefficient [9]. As shown by Lange [6], this method guarantees sufficient precision.

In practice hydrocarbon/water blends are frequently used as the immiscible material combination. For this reason we selected *n*-heptane and water as vapours for these experiments because their liquids have a negligible degree of miscibility. Furthermore they are safe and easy to handle and have been used before in other tests under atmospheric pressure conditions, so comparisons are available. Nitrogen is used as the non-condensing gas.

Finally the objectives can be summarized as follows:

- Presentation of test results at increased pressure ( $1 \text{ bar} < p < 10 \text{ bar}$ ) and high gas ( $Re_G > 25\,000$ ) and liquid flow rates ( $Re_L > 150$ ).
- Examination of existing methods of calculation for the description of the coupled heat and mass transfer in the gas phase.
- Examination and possible expansion of models for calculating heat transport in the condensate film.

## 2. PHASE EQUILIBRIA

The miscibility of many combinations of organic material and water is negligible. This means that the activity coefficient of the components  $\gamma_i = 1$  apply, i.e. virtually total immiscibility can be assumed. If there is a further, non-condensing component in the mixture, the condensation procedure can be described in a triangular diagram (figure 1) according to Deo [2] and a temperature composition diagram (figure 2). The material combination *n*-heptane with water, and non-condensing gas  $N_2$  are used.

The special quality of this system is the existence of a heteroazeotrope or, in analogy with a solid/liquid system, usually called a eutectic state. The line through points  $E_1$ , E and  $E_2$  in figures 1 and 2 are called eutectic lines. Only when there are compositions at the gas/liquid boundary, which lie on these lines, can all three phases ( $\Phi = 3$ ) be in equilibrium. Therefore, in this case the ternary system ( $l = 3$ ) has, in accordance with the phase rule of Gibbs

$$fr = 2 + l - \Phi \quad (1)$$

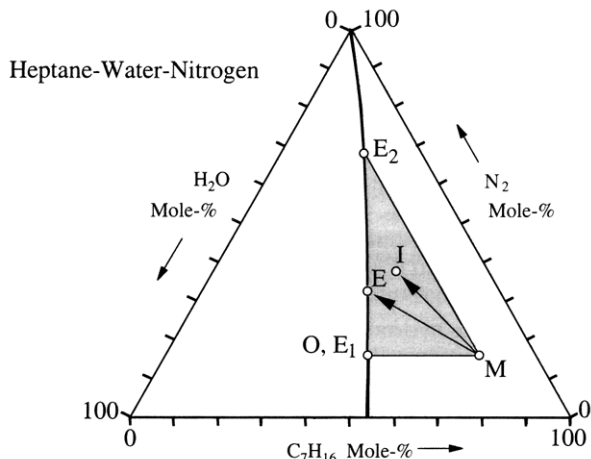


Figure 1. Ternary diagram of a binary vapour mixture, completely immiscible in the liquid state, in the presence of a noncondensable gas.

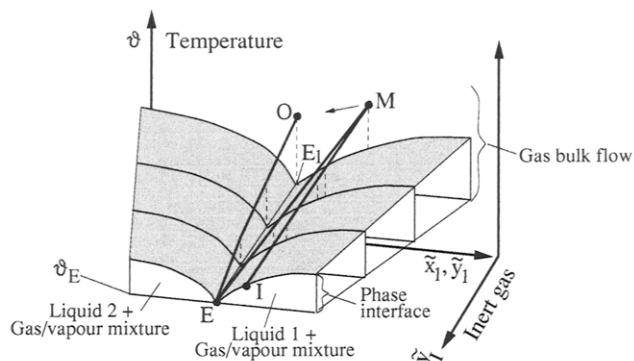


Figure 2. Boiling point diagram of a binary mix, completely immiscible in the liquid state, in the presence of inert gas.

two degrees of freedom. The eutectic temperature can be calculated in this way at the given pressure  $p$  and proportion of inert gas  $\tilde{y}_I$  from the vapour pressures  $p_i^\circ$  of the two vapours.

$$p_1^\circ(T_e) + p_2^\circ(T_e) = p(1 - \tilde{y}_I) \quad (2)$$

If there is a situation on the right side of the eutectic line, e.g. point M, only the heptane component will be condensed. If the situation is on the left, only water will be condensed. In the case of point M, depending on the hydrodynamic and cooling conditions, situations can only arise on the phase boundary lying in the  $E_1 ME_2$  area. Lines  $E_1 M$  and  $ME_2$  are parallel to the axes in each case.

In principle two compositions can occur during the gas phase.

- 1) The composition of the gas phase represents the eutectic as shown in figure 2,  $E_1$  or O.
- 2) The composition of the gas phase is not equal to the eutectic, e.g. at point M.

Based on these two cases it is possible to show three different condensation processes in figure 1. The effect of the temperature can also be seen in the boiling point diagram in figure 2.

1) If a gas/vapour mixture with eutectic composition is available and the phase boundary temperature is lower than the eutectic temperature  $\vartheta_e$ , both vapours will condense simultaneously. The process runs with a set composition of vapour and liquid mixture (line  $E_1 E$ ). The diffusional resistance in the gas phase is exclusively dependent on the proportion of non-condensing gas, and the condensation is similar to the condensation of one pure vapour with a non-condensing gas.

2) Based on a non-eutectic composition (point M), when the phase boundary temperature is lower than the boiling temperatures of the pure substances and above the eutectic temperature  $\vartheta_e$ , only one component (line MI) will condense. Meanwhile the other behaves like a non-condensing gas and therefore strengthens the mass transfer resistance of the gas.

3) If the temperature drops below  $\vartheta_e$  both vapours will condense simultaneously (line ME). Here the composition of the liquid phase and the quantity of the condensate mass flow depends mainly on the rate of mass transfer.

The condensation of an superheated gas/vapour mixture in a non-eutectic state by countercurrent cooling is the usual industrial condition. When a mixture of this kind enters the condenser and if the surface temperature of the condensate formed on entry is around point I in *figure 2*, only component 1 will condense initially. The diffusional resistance between the two vapours decreases constantly along the condenser length. Therefore, by further condensation, the state of the gas will move from point M in the direction of point E<sub>1</sub>. Condensation also causes a decrease of the phase boundary temperature and, for this reason, the state of point I will shift towards point E. When the stable eutectic state E has been reached, condensation will take place in accordance with point 3 above.

### 3. HEAT TRANSFER IN THE LIQUID PHASE

#### 3.1. Forms of condensate

During condensation of vapours of immiscible liquids, the structure of the condensates produced is usually completely different from that in miscible or pure liquids. Because these forms are very complex, it has not yet been possible to produce a complete hydrodynamic model.

Basic theoretical work and visual experiments of this kind of condensation were previously carried out by Bernhardt et al. [3], Akers and Turner [4], Marmai [10], Polley and Callus [11], and more recently by Hoon and Burnside [12], Hayashi et al. [13], as well as in one of our own studies [14]. All the authors base the description of their surveys on two fundamental forms of condensation – filmwise condensation and dropwise condensation (*figure 3a,b*).

If a condensed substance has only low interfacial tension in the liquid state relative to the surface material, a continuous film will be formed spontaneously, whereas in the case of materials with high surface tension, e.g. water, dropwise condensation will take place from the start of the condensation process. In the latter case, at a higher condensation rate, the drops will coagulate to form streams and eventually film condensation will be obtained. Calculation of the heat conduction resistance in film condensation is more or less reliable and is based, e.g. in the case of laminar flow conditions, on the Nusselt layer theory [15].

Heat transfer rates in dropwise condensation are considerably higher. Calculation of this is, however, extremely complex because both the nucleation site density and also the drop radius are difficult to predict.

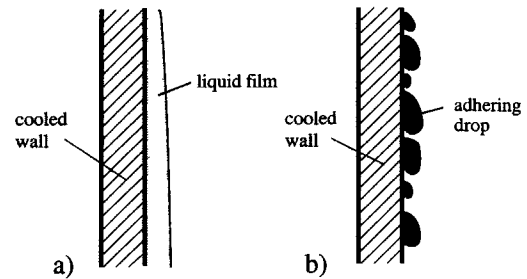


**Figure 3.** Basic forms of condensation: a: filmwise condensation; b: dropwise condensation.

If there is a combination of both basic forms of condensation, the heat transfer rate can be expected to be higher than that produced by filmwise condensation.

Bernhardt [2] made his observations at low condensation rates with drops of water sticking to a vertical, plain copper plate with an organic film flowing around them (see *figure 4*, right hand side). The drops are in contact with the vapour phase and therefore grow continuously until, when a critical size has been reached, they run down the wall, partly due to the shearing forces of the film or the vapour flow, and partly due to the force of gravity. In addition to this, small lenticular water drops swimming on the film and extremely small organic drops moving at high speed on the surface of the drops of water were observed. Studies of longer condenser surfaces, interesting for industrial applications, as made by Polley and Callus [7] or Hayashi et al. [8] have been confirmed in principle by our own experiments. The surface can be divided into zones with fluid boundaries as shown on the left hand side of *figure 4*.

– The top section comprises mainly dropwise condensation of the water vapour with a very thin heptane film on the surface area where there are no drops. The drops of water grow by absorbing water condensate and run down the wall, partly due to their weight and partly due to the shearing force of the thickening organic film.

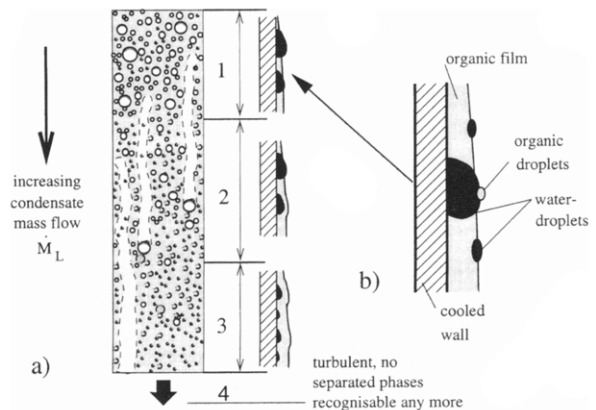


**Figure 4.** Qualitative forms of condensation: a: our own study [2]; b: study of Bernhardt et al. [3].

- In the central section, the area wiped clean by drops of water running down, is quickly covered again by drops of water growing in size and sticking to the surface.

- In the lower section the drops of water no longer protrude from the thicker organic film. Surfaces wiped clean are sparingly covered with new drops of water. Both condensed liquid components are mixed within the film.

- Separate phases can no longer be identified at higher condensate mass flow rates with  $Re_L \approx 100$ . The condensate rushes turbulently, in strong waves, down the wall.

Depending on the working conditions, the forms of condensation shown in *figure 4* can occur simultaneously, making it difficult to determine where the transition boundaries are. Due to this complex combination of different forms it seemed to be necessary to produce a stage model for calculation of the heat transfer rate.

### 3.2. Heat transfer calculation

These visual examinations produced a number of diverse models as a basis for calculation of heat transfer in the condensate. The models from Bernhardt et al. [2] and Akers and Turner [3], as already mentioned, obtain satisfactory conformity with previously known data by means of fairly simple equations.

- The *Shared surface model* in [2] works on the assumption that when segregation occurs during condensation, defined channels are formed in which the separate components flow down the wall. In each case the channels coat that part of the surface area of the condenser which is equal to the proportional volume  $\hat{x}_i$  of the components in the condensate. Therefore the heat transfer coefficient  $\alpha$  of the mixture is composed of the coefficient of the pure components measured by volume.

$$\alpha_L = \sum_n^{i=1} \hat{x}_i \alpha_{L,i} \quad (3)$$

- The *Homogeneous liquid model* in [3] was developed from the theory that two components will flow down within a film in the form of a homogeneous, dispersed mixture or as an emulsion of lenticular drops according to their mutual coating. To calculate the heat transfer coefficients with reference to the soluble components, averaged data for the properties of the two components and the viscosity of the component coating the wall were applied.

As the flow rate of condensate in an immiscible system under previously unexamined, but technically relevant working conditions, is frequently turbulent, a method developed by Müller [16] for calculation of the condensate Nusselt number has been integrated into

the calculation. This is based on the existence of two temperature gradients in the condensate, as shown in *figure 5*, and presents a series addition of the transfer resistances he discovered in the vicinity of the wall and liquid surface areas.

$$\frac{1}{Nu_L} = \frac{1}{Nu_{L,W}} + \frac{1}{Nu_{L,O}} \quad (4)$$

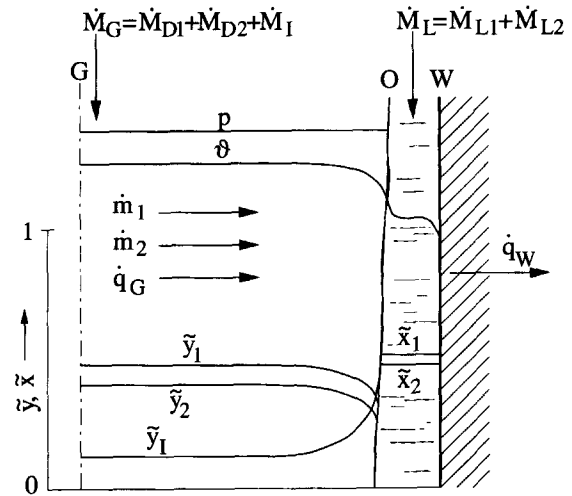


Figure 5. Example radial temperature and concentration profiles during partial condensation of a eutectic gas/vapour mixture in a tube.

Furthermore, as was shown by Müller [16], Nusselt numbers exist for laminar and turbulent liquid flow conditions in the vicinity of the wall and surface areas. They are summed in the following way:

$$Nu_{L,W} = \sqrt[4]{Nu_{L,W,lam}^4 + Nu_{L,W,tur}^4} \quad (5)$$

In analogy to this the Nusselt number for the surface areas  $Nu_{L,O}$  is created. Since it is expected that the condensate will be exposed to significant shearing stress caused by the gas phase, an Andreussi [17] method, which produced good results in the studies carried out by Claus [7] and Hadley [8] amongst others, is used here.

Following our own experiments, an intensive mixing of the components caused by the turbulent liquid downward stream was observed in the range of higher condensate mass flow rates. This seems to make the application of a theoretical model of homogeneously mixed condensate and the calculation methods deduced from this by Akers and Turner preferable, particularly under technically relevant working conditions at high condensate flow rates.

## 4. HEAT AND MASS TRANSFER IN THE GAS PHASE

During the condensation process the composition of the gas/vapour mixture and the hydrodynamic conditions along the condenser tube undergo continuous change. It is, therefore, necessary to make a step-by-step calculation of the process using local variables of state and transport. *Figure 5* shows typical temperature and concentration gradients during condensation of a gas/vapour mix of azeotropic or virtually azeotropic composition flowing through a vertical pipe.

The differences in concentration between the bulk flow of the gas/vapour mixture G and the surface area of the condensate I produce the mass fluxes  $\dot{m}_1$  and  $\dot{m}_2$ , which are perpendicular to the wall. If, in contrast to *figure 5*, the gas/vapour mixture is non-eutectic and the surface temperature of the film is higher than the eutectic temperature, only one component will be condensed. It follows that in this case one  $\dot{m}_i$  equals zero and the non-condensing component is added to the non-condensing gas as imposing mass transfer resistance.

A heat flux  $\dot{q}_G$ , caused by the evaporation enthalpy released at the phase boundary and decrease of temperature in the gas phase, must be carried through the condensate via the tube wall to the cooling water. The film surface temperature, for which there is no suitable measurement technique, is required for calculation of the heat flux which is normal to the wall in the gas and liquid phases, as well as for the mass flux corresponding to this. They are calculated by means of an energy balance on a volume element of the condensate flowing down the wall. If the heat flux via the wall  $\dot{q}_w$  is set equal to the heat flux through the condensate  $\dot{q}_L$ , the following is produced for small step sizes  $\Delta z$ :

$$\begin{aligned} \alpha_L (\vartheta_O - \vartheta_W) &= \alpha_G (\vartheta_G - \vartheta_O) \\ + \dot{m}_1 (\Delta h_{V1}(\vartheta_O) + \bar{c}_{pL1} \vartheta_O) + \dot{m}_2 (\Delta h_{V2}(\vartheta_O) + \bar{c}_{pL2} \vartheta_O) \\ - (\dot{m}_1 \bar{c}_{pL1} + \dot{m}_2 \bar{c}_{pL2}) \vartheta_L - \left( \frac{\dot{M}_{L1}}{\pi d} c_{pL1} + \frac{\dot{M}_{L2}}{\pi d} c_{pL2} \right) \frac{\Delta \vartheta_L}{\Delta z} \end{aligned} \quad (6)$$

The unknown film surface temperature can now be determined iteratively by giving a starting value and suitable rates for the heat transfer coefficients in the gas and liquid phases  $\alpha_G$  and  $\alpha_L$  as well as the mass fluxes  $\dot{m}_i$ .

The heat transfer coefficient  $\alpha_G$  between the bulk flow of the gas/vapour mix  $\vartheta_G$  and the phase boundary  $\vartheta_I$  is calculated by means of a modified Nusselt-regression equation in accordance with Numrich [18].

$$\begin{aligned} Nu_G &= \frac{\alpha_G L_G}{\lambda_G} \\ &= \frac{\xi_g}{8} \frac{(Re_G^* - 1000) Pr_G \xi_r / \xi_g}{1 + 12.7 \sqrt{\xi_g/8} ((Pr_G \xi_r / \xi_g)^{2/3} - 1)} C_q f(d/z) \end{aligned} \quad (7)$$

In this equation the shearing stress caused to the condensate by the gas flow as the friction correction values  $\xi_g$  and  $\xi_r$  in accordance with [16] is considered. In the same way the unsteady flow at the beginning of the condenser tube is included as the correction factor  $f(d/z)$  and the effect of the one-sided diffusion by the correction factor  $C_q$  according to Ackermann [19].

The mass flux rates  $\dot{m}_1$  and  $\dot{m}_2$  can be calculated from the difference in concentration during the gas phase in one cross section.

$$\dot{m}_i = \beta_{G,i} c_G \tilde{M}_i (\tilde{y}_{i,G} - \tilde{y}_{i,O}) \quad (8)$$

The Sherwood-number is used for calculating the mass transfer coefficients in the gas phase  $\beta_G$ . These are formed by analogy to the Nusselt number in equation (7).

$$\begin{aligned} Sh_{G,i} &= \frac{\beta_{G,i} L_G}{D_{i,m}} \\ &= \frac{\xi_g}{8} \frac{(Re_G^* - 1000) Sc_{G,i} \xi_r / \xi_g}{1 + 12.7 \sqrt{\xi_g/8} ((Sc_{G,i} \xi_r / \xi_g)^{2/3} - 1)} C_{m,i} f(d/z) \end{aligned} \quad (9)$$

Factor  $C_{m,i}$  includes the compensating flow caused by partial condensation. The diffusion coefficient of the components in the gas/vapour mixture is determined by the method based on an *effective diffusion coefficient* developed by Wilke [9] from the individual, binary diffusion coefficients  $D_{ij}$ . Here it is simply assumed that all components, other than those under scrutiny, are at rest.

$$D_{i,m} = \frac{1 - \tilde{y}_i}{\sum_{j=1, j \neq i}^k \tilde{y}_j / D_{ij}} \quad (10)$$

It was possible to demonstrate in studies, e.g. from Lange [6], who considers vapour mixtures of miscible liquids under similar conditions, that this method is sufficiently precise.

## 5. EXPERIMENTS

### 5.1. Experimental plant

*Figure 6* shows the unit used for the main experiments carried out at above atmospheric pressure. Controlled quantities of the vapours are mixed with the heated non-condensing gas and the mixture is slightly superheated when it reaches the top of the measuring section (shown in detail on the right hand side of *figure 6*). This measuring section comprises a 3.1 m

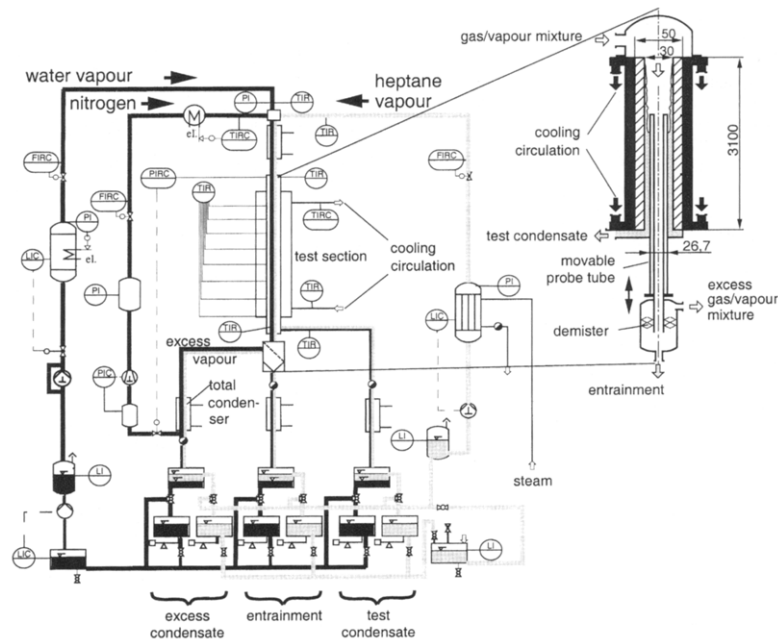


Figure 6. Diagram of the plant used for partial condensation of two vapours at increased pressure.

long brass pipe with an outside diameter of 50 mm and a wall thickness of 10 mm. A countercurrent stream of cooling water flows around the outside of the pipe. The vapours are partially condensed on the inside wall of the pipe and flow down the wall in co-current flow with the gas phase. Inside the measuring pipe there are 4 NiCr–Ni thermocouples of 0.5 mm diameter, soldered at each of 8 levels on opposite sides of the pipe to measure the inside and outside wall temperature. The local heat flux can be determined in this way. The length of the cooling section can be adjusted by a vertical, infinitely variable probe tube. The experimental plant described here and, in particular, the measuring section, can be used for experimental examination of film condensation in a vertical pipe based on the integral measuring principle. This principle provides that, under stable inlet conditions and by varying the position of the mobile probe tube, the amount of condensate flowing along the cooling section  $z$  can be measured experimentally.

Characteristics of the inlet conditions are:

- 1) mass flow rates of the vapours and non-condensing gas
- 2) composition of the gas/vapour mixture
- 3) temperatures of the gas/vapour mixture
- 4) cooling conditions
- 5) pressure.

The quantity of condensate, measured in this way, flows down the wall in a circular gap between the probe and the measuring pipe. The residual gas/vapour mixture flows down together with any entrainment on the inside of the sensor tube. When the drops

of liquid have been separated out, the remaining vapour is completely condensed and a settler tank is added to each of the three emulsion flows – residual condensate, entrainment and measured condensate. The two components are separated in the settler due to their different densities. The individual mass flow rates are measured gravimetrically by diverting the flows into weighing vessels. The mass flows are subsequently transferred to storage tanks from which the quantities required for the evaporator are then extracted. After complete condensation of the residual vapours, the non-condensing gas leaves the condenser through a valve which regulates the plant pressure. It is then processed, compressed, cleaned and supplied again to the mixing chamber in regulated quantities.

In addition to the wall temperatures and condensate mass flow rates, measurements are also taken of the system pressure, inlet mass flow rates of the gas and vapours, and also temperatures at the inlet to the measuring section, on the top of the probe tube, which is the outlet for the residual gas/vapour mixture, and the inlet and outlet cooling medium temperatures.

## 5.2. Experimental conditions and realization

The results of the experiments presented here were obtained under the conditions which are cited in the table.

Each of the series of measurements was completed using 5 measuring points at the cooling section lengths

TABLE Experimental conditions.	
Number of experimental series	
Eutectic inlet conditions	26
Non-eutectic inlet conditions	37
Measuring tube inlet	
Pressures	$p = 5$ and $9$ bar
Mole fraction of the inert gas	$\tilde{y}_I = 0.2, 0.5, 0.8$ (0.3)
- eutectic experiments	$\tilde{y}_I = 0.2, 0.35, 0.5$
- non-eutectic experiments	$\vartheta_C = 40, 70, 100$ °C
Cooling temperatures	
Total mass flow rate	
- eutectic experiments	$\dot{M}_E = 100, 200$ (150) $\text{kg}\cdot\text{h}^{-1}$
- non-eutectic experiments	$\dot{M}_E = 100 - 192$ $\text{kg}\cdot\text{h}^{-1}$
Temperature in the gas phase	$\vartheta_{G,E} = 77.5 - 141.7$ °C
Reynold number in the gas phase	$Re_{G,E} = 85\,000 - 239\,000$
Measuring tube outlet	
Condensate Reynold number	$Re_L = 140 - 1\,070$
Condensate Prandtl number	$Pr_L = 3.5 - 5.5$

$z = 0.5; 1.05; 1.65; 2.25; \text{ and } 2.85$  m while the inlet conditions were kept constant. After the measuring point had been reset the condensate mass flow rates were measured to determine when a steady state had been reached. When 3 almost identical massflow readings had been obtained, these were averaged arithmetically and, by moving the probe tube, the next measuring point was set.

### 5.3. Experimental results and discussion

A great number of measured data were digitalised by an A/D converter and logged by a data processing program to document the experimental conditions described above. While measurements were being taken at each of the cooling lengths  $z$ , the data was being processed by the program and, on completion of the measuring process, a data table was printed. *Figure 7* shows a typical series of experiments with eutectic inlet conditions.

As already mentioned, the behaviour of a mixture with eutectic composition during condensation can be equated with the partial condensation of a pure vapour. The calculation methods used for mass and heat transfer, and to determine the shearing force between gas and condensate mass flows, have been formulated, sufficiently examined and validated by studies produced by Numrich [18, 20], Lange [6], Claus [7] and Hadley [8].

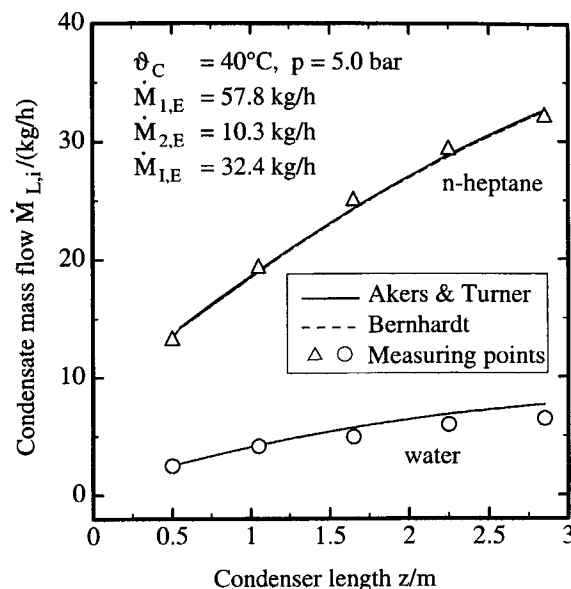


**Figure 7.** Comparison of measured and calculated condensate massflow rates for the individual components of an eutectic inlet mixture.

For this reason comparison shows good to very good agreement between the calculation and measured data as can be seen in *figure 7*.

It can also be clearly seen here that no difference is evident between the two models produced by Bernhardt and Akers and Turner for calculation of heat transfer in the liquid phase. This indicates that even at an average non-condensing gas mole fraction of 0.5, as in the experimental series presented here, the mode of calculation of the liquid phase does not play a significant role. Only in the case of experiments using a small non-condensing gas concentration of  $\tilde{y}_I = 0.2$ , and at the lower pressure of 5 bar, can a small difference between the two methods of calculation be perceived. In this connection, the method used by Akers and Turner is higher and closer to the measured data in each case than the method used by Bernhardt et al. With experiments carried out at 9 bar and  $\tilde{y}_I = 0.2$  only a very slight difference can be distinguished, but the heptane flux is undercalculated also in experiments at high cooling water temperatures, i.e. 100 °C. So the calculated total condensate flow rates are about 20 % lower than the measured.

If carefully controlled inlet conditions relatively far away from the eutectic composition are set, greater differences will be identified between the calculated and the measured data. In *figure 8* this is clearly demonstrated in the condensate flow rates.

In this experimental run, as in all experiments with surplus of water, as opposed to the experiments with eutectic compositions, the calculated condensate mass flow rates are considerably higher than those obtained in eutectic experiments. Furthermore, it is



noticeable that the curves calculated for the water condensate are again almost all higher than the water condensate measurements. This leads to an excessively high estimation of the total condensate mass flow and, at the same time, an under-prediction of the bulk temperature in the gas phase.

In figure 8 it is clearer to see than in the eutectic experiments that the Akers and Turner methods predict lower condensate flow rates. In this case they are closer to the measured values than those produced by the Bernhardt method, and this applies to the full series of non-eutectic experiments.

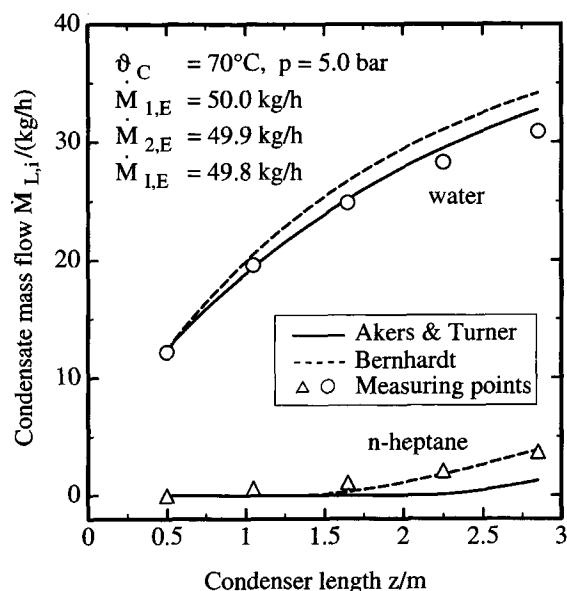


**Figure 8.** Comparison of measured and calculated condensate massflow of individual components of a non-eutectic inlet composition of surplus water.

If, for example, an inlet mixture with a surplus of heptane is selected, the predicted condensate mass flow rates are just below the measured values as in the eutectic experiments. Furthermore, in a similar manner to the eutectic experimental series, there is only a small difference, if any, between the methods of calculation provided by Bernhardt and Akers and Turner.

In order to carry out a uniform assessment of the tests which have been performed, the theoretical mass flow difference of the total condensate  $\Delta \dot{M}_{L,th}$  between the max. cooling section length  $z = z_{max} = 2.85$  m and the starting point  $z_0 = 0.5$  m is calculated and applied to the experimentally calculated mass flow difference  $\Delta \dot{M}_{L,exp}$ .

$$\Delta \dot{M}_{L,th} = \dot{M}_{L,th}(z_{max}) - \dot{M}_{L,exp}(z_0) \quad (11)$$

$$\Delta \dot{M}_{L,exp} = \dot{M}_{L,exp}(z_{max}) - \dot{M}_{L,exp}(z_0) \quad (12)$$

In addition, the only test results available from the literature for condensation of an immiscible mixture

under the influence of a non-condensing gas are included in the diagram. These were reported by Sardesai [1] in systematic experiments but at much lower condensate mass flow rates. It is noticeable here that previous experiments, as mentioned above, have been carried out exclusively on a laboratory scale, meaning that the scale-up of results to industrial conditions is limited.

It is also obvious that the measurements obtained from experiments with eutectic compositions are well predicted, within a range of variation between +20 % and -28 % (figure 9).

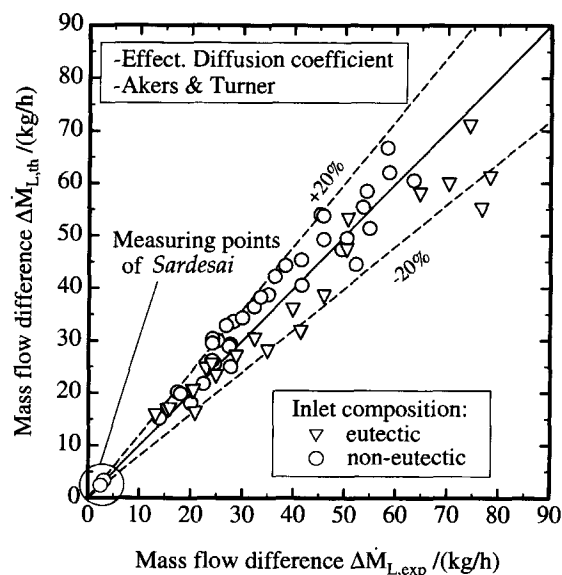


**Figure 9.** Comparison of the experimentally and theoretically calculated total condensate massflow difference  $\Delta \dot{M}_L$  using the effective diffusion coefficient and condensate heat transfer determined by the Akers and Turner method [4].

However, in contrast to that, it is clear that the experiments with non-eutectic mixtures have been systematically over-predicted. Because of the physical properties of the vapour components (eut. point:  $x_{water} \approx 0.13$ ,  $x_{heptane} \approx 0.87$  at 1 bar), the non-eutectic mixtures usually have a surplus of water. The experiments with excess heptane are, in contrast with these measurements, underpredicted. One cause of the systematic variation could be the method by which the mass transfer is calculated. Mass transfer processes in the case of non-eutectic compositions are far more complex due to the difference in the concentration gradient of the two vapours. As opposed to eutectic mixtures, the binary diffusion coefficient *n*-heptane/water plays a more important role in this case. This value is, however, relatively unsafe due to the varying polarities of the two vapour components calculated by the method proposed in the literature [21]. There is a further inaccuracy in the method of calculating the effective diffusion coefficient which is oversimplified under the prevailing conditions.

But, on the other hand, in the eutectic experiments where this diffusion coefficient is irrelevant for the mass transfer determination, the same undercalculation of the mass fluxes occurs.

This means that, as in this case, the transport processes mentioned above are relatively simple, in comparison to those for partial condensation of a pure vapour, the calculations of the coupled heat and mass transfer in the gas phase can be considered satisfactory.

The main reason for this systematic overdetermination of the water mass flow rate and underdetermination of the heptane mass flow rate is the uncertain heat transfer calculation through the individual condensate components under these hydrodynamic conditions.

Therefore the next step for us is a more detailed investigation of the heat transfer in turbulent flowing films of emulsions.

## 6. CONCLUSION

Experiments on partial condensation of vapours of two immiscible liquids with a non-condensing gas were, before now, carried out exclusively at very limited flow rates and at a laboratory scale, i.e. under atmospheric pressure and at low mass flow rates. The gas phase in those experiments was, at its highest flow rate, in the lower turbulence range, whereas the liquid phase was exclusively laminar.

During these studies, partial condensation was examined in a brass pipe of 30 mm inside diameter in a co-current downwards flow at higher pressures, up to 9 bar. Experimental conditions, previously not examined for this system, could be established and maintained.

- $p = 5$  to 9 bar
- $Re_{G,E} = 85\ 000$ –239 000
- $Re_{L,A} = 140$ –1 050

The hydrodynamic state in the gas phase is within the turbulent flow range, whereas laminar to turbulent flow conditions are achieved in the condensate flowing down the wall.

The two best methods described in the literature up till now were used to calculate heat transfer in the condensate. Both the correlations described by Akers and Turner [4] and by Bernhardt et al. [3] are based on calculation methods developed from model concepts in accordance with observed forms of condensate (homogeneous or separated flows respectively). However, until now, these have only reflected the data obtained under the laboratory conditions described above.

To interpret the condensate flow structures, only observed at discrete points by previous authors, and to achieve scale-up of the experiments, we carried out our own experiments in a laboratory unit. These confirmed the visual results of other authors and the change to

other forms of condensation could be shown. At higher condensate mass flow rates, increasingly thorough mixing of the two liquid components was observed. This seems to make the applicability of the model based on homogeneously mixed condensate in accordance with Akers and Turner [4] and the resultant calculation method more appropriate, especially under technically relevant working conditions at high condensate flow rates.

Finally experiments with a vapour mixture of *n*-heptane/water and nitrogen as non-condensing gas were performed in the main experimental plant, at a wider range of parameters than used in previous works. These were carried out initially at a range of increased pressures and related higher gas and condensate mass flow rates as frequently produced in industrial units.

To allow comparisons of experimental with predicted results, software was developed to work with an integral calculation principle using local mass and heat transfer coefficients. This provided the possibility of integrating different methods of calculation of individual partial processes to demonstrate their applicability. Using the comparison of calculation and experiment it was possible to report that:

1) It is possible to use simple methods of calculation from model concepts (homogeneously mixed or channeling flow) for calculation of the heat transfer of two-phase condensates with sufficient accuracy, over all the tested conditions. In practice only small differences could be found between the results of the two methods. In general, however, the results produced by an homogeneously mixed model in accordance with Akers and Turner were closer to the measured data, in particular in the case of non-eutectic inlet mixtures.

2) Safe correlations to predict the coupled heat and mass transfer in the gas phase, bearing in mind the real behaviour in the gas phase and effect of higher shear stresses on the condensate, can be transferred without reservation to a system with eutectic compositions or even to a system where the inlet compositions are slightly different. In the case of non-eutectic compositions there are slightly larger variances from the measured data as, in this case, there is increased complexity of the mass transfer processes. In the eutectic experiments the previously calculated condensate mass flow rates correlate the experimental results at a precision of +20 % to –28 %. In non-eutectic experiments, the calculated condensate mass flow rates vary between +26 % to –15 % in comparison to the measured values. These different deviations are caused by a systematic slight overprediction of the water condensate flow together with an underprediction of the heptane mass flow.

## REFERENCES

- [1] Sardesai R.G., Studies in condensation, Thesis, University of Manchester, UK, 1979.

- [2] Deo P.V., Condensation of mixtures of vapours, Thesis, University of Manchester, UK, 1979.
- [3] Bernhardt S.H., Sheridan J.J., Westwater J.W., Condensation of immiscible mixtures, American Institute of Chemical Engineers, Symp. Ser. 68 (1972) 21–37.
- [4] Akers W.W., Turner M.M., Condensation of vapours of immiscible liquids, *AIChE J.* 8 (1962) 587–589.
- [5] Sardesai R.G., Condensation of vapor mixtures forming immiscible liquids, *Heat Exchanger Design Handbook*, Hemisphere Publishing Corp, 1983.
- [6] Lange J., Die partielle Kondensation zweier im flüssigen Zustand löslicher Komponenten aus einem Gas/Dampf-Gemisch im senkrechten Rohr bei erhöhtem Druck, Thesis, Universität-GH Paderborn, 1994.
- [7] Claus N., Kondensation strömender reiner Dämpfe im senkrechten Rohr bei Drücken bis 15 bar, Thesis, Universität-GH Paderborn, 1996.
- [8] Hadley M., Kondensation binärer Dampfgemische unter dem Einfluss der vollturbulenten Gasströmung bei Drücken bis 13 bar, Thesis, Universität-GH Paderborn, 1996.
- [9] Wilke C.R., Diffusional properties of multicomponent gases, *Chem. Eng. Progr.* 46 (1950).
- [10] Marmai U., Zum Mechanismus der Kondensation binärer Dampfgemische mit nichtmischbaren Komponenten im flüssigen Zustand, *Wissenschaftl. Zeitschrift der TH Karl-Marx-Stadt XVIII (5)* (1978).
- [11] Polley G.T., Callus W.F., Condensation of binary mixtures of vapours of immiscible liquids with channeling flow of the condensate, in: *Proceedings of the 7th International Heat Transfer Conference, Munich, 1982*, vol. 5, pp. 195–203.
- [12] Hoon J.H., Burnside B.M., Condensation of the Stear/Nonane system on a vertical flat plate and a single column of horizontal tubes, in: *Fundamentals of phase change: boiling and condensation, AIAA/ASME conference, Seattle, Washington, 18–20 June 1990*, pp. 55–62.
- [13] Hayashi H., Takimoto A., Teranishi T., Condensation of binary vapours of immiscible liquids, in: *Proceedings of the Engineering Foundation Conference on Condensation and Condenser Design, Saint Augustine, USA, 1993*.
- [14] Mönning C., Kondensation eines im flüssigen Zustand unlöslichen Dampfgemisches, Diplomarbeit, Universität-GH Paderborn, 1993.
- [15] Nusselt W., Die Oberflächenkondensation des Wasserdampfes, *VDI Zeitung* 60 (1916) 541–546 & 569–575.
- [16] Müller J., Wärmeübergang bei der Filmkondensation und seine Einordnung in Wärme- und Stoffübertragungsvorgänge bei Filmströmungen, Thesis, TH Karlsruhe, 1992.
- [17] Andreussi P., The onset of droplet entrainment in annular downward flows, *Can. J. Chem. Eng.* 58 (4) (1980) 267–270.
- [18] Numrich R., Stoff-, Wärme- und Impulsaustausch bei der Kondensation von Ein- und Mehrkomponentensystemen, Habilitationsschrift, Universität-GH Paderborn, Verlag Shaker, 1995.
- [19] Ackermann D., Wärme- und Stoffaustausch bei der Kondensation eines turbulent strömenden Dampfes in Anwesenheit von Inertgas, Thesis, 1972.
- [20] Numrich R., Die partielle Kondensation eines Wasserdampf/Luftgemisches im senkrechten Rohr bei Drücken bis 21 bar, Thesis, Universität-GH Paderborn, 1987.
- [21] Weiss S. (HRSG), Verfahrenstechnische Berechnungsmethoden, Teil 7, Stoffwerte, VCH Verlagsgesellschaft, Weinheim, 1986.
- [22] Mönning C., Numrich R., Partial condensation of binary vapours of immiscible liquids, in: *Proceedings of the 47th Eurotherm Seminar, Paris, France, 03–06 October 1995, ADEME (Agence de l'environnement et de la maîtrise de l'énergie)*.

